Selection of chemotactic adipose-derived stem cells using a microfluidic gradient generator

Natarajan, Kanmani; Tian, Chantal; Xiang, Bo; Chi, Chao; Deng, Jixian; Zhang, Rundi; Freed, Darren H.; Arora, Rakesh C.; Tian, Ganghong; Lin, Francis

Publisher's version / Version de l'éditeur:
https://doi.org/10.1039/C4RA12863J
RSC Advances, 5, 9, pp. 6332-6339, 2014-12-22

RSC Advances

PAPER

View Article Online
View Journal | View Issue

Cite this: *RSC Adv.*, 2015, **5**, 6332

Selection of chemotactic adipose-derived stem cells using a microfluidic gradient generator†

Kanmani Natarajan,[ab] Chantal Tian,[a] Bo Xiang,[cd] Chao Chi,[def] Jixian Deng,[df] Rundi Zhang,[a] Darren H. Freed,[g] Rakesh C. Arora,[h] Ganghong Tian*[df] and Francis Lin*[abij]

Stem cells hold great promise for treating various degenerative diseases and conditions. However, the outcomes of preclinical and clinical cell therapy studies are still not close to our expectation. We believe that the unsatisfactory outcomes of cell therapy are at least partially due to insufficient homing of implanted stem cells into target organs and the use of heterogeneous cell populations for cell therapy. Therefore, there is a need to develop an effective guiding technique for stem cells to migrate to the target organs and to isolate effective stem cell populations. Toward this direction, we have previously demonstrated chemotaxis of rat adipose-derived stem cells (ASCs) to a well-defined gradient of epidermal growth factor (EGF) using a microfluidic device. In the current study, we further developed a microfluidics-based method for selecting chemotactic ASCs to EGF. This method integrates cell patterning, chemotaxis and cell extraction on a single microfluidic gradient-generating device. Post-extraction analysis confirmed the higher chemotactic migration of the extracted cells to EGF. Consistently, the extracted chemotactic ASCs shows up-regulated surface expression of the EGF receptor and its downstream signaling event upon EGF stimulation. The results suggest that our method provides a new effective approach for the selection of specific stem cell populations. It is also expected that the use of the selectively extracted stem cells could enhance stem cell homing to target organs and consequently improve the outcome of cell therapy.

Received 21st October 2014
Accepted 8th December 2014

DOI: 10.1039/c4ra12863j

www.rsc.org/advances

Introduction

Stem cells are one of the key building blocks for tissue regeneration because of their self-renewal ability and multi-potential to differentiate into different specialised cell types such as cardiomyocytes, blood cells and nerve cells.[1–4] Adult stem cells can be isolated from various tissue sources.[5] Among the adult stem cells, adipose derived stem cells (ASCs) are a type of mesenchymal stem cells derived from fat tissues.[6–9] ASCs have extensive proliferative capacity and can differentiate into multiple cell lineages.[10–12] Moreover, a significant amount of adipose tissue can be readily harvested with a minimal invasive procedure without provoking ethical concerns and prolonged *ex vivo* expansion.[7,13,14] These unique features make ASCs a promising stem cell source for transplantation-based therapeutic applications.[8,12]

Homing of transplanted stem cells to the targeted tissues depend on various factors such as the cell conditions, the host conditions and the delivery method.[15] Our previous study showed that direct injection of ASCs into injured myocardium significantly increased left ventricular ejection fraction and reduced infarct size of infarcted rat hearts.[12] Therefore, we believe that ASCs is an effective candidate for treating congestive heart failure and other degenerative diseases. Most stem cell-based therapeutic studies, particularly human ones, have only shown very moderate improvement of viability and function of targeted tissues and organs. We anticipate that the unsatisfactory outcomes of the studies were at least partially due to the insufficient homing of the implanted stem cells to

[a]*Department of Physics and Astronomy, University of Manitoba, Winnipeg, MB, R3T 2N2, Canada. E-mail: flin@physics.umanitoba.ca*

[b]*Department of Biological Sciences, University of Manitoba, Winnipeg, MB, R3T 2N2, Canada*

[c]*Department of Pharmacology and Therapeutics, University of Manitoba, Winnipeg, MB, R3E 0T6, Canada*

[d]*National Research Council, Winnipeg, MB, R3B 1Y6, Canada. E-mail: Ganghong.Tian@nrc-cnrc.gc.ca*

[e]*Department of Cardiac Surgery, The First Affiliated Hospital, Harbin Medical University, Harbin, China*

[f]*Department of Physiology and Pathophysiology, Faculty of Medicine, University of Manitoba, Winnipeg, MB, R3E 0J9, Canada*

[g]*Division of Cardiac Surgery, University of Alberta Hospital, Canada*

[h]*Cardiac Science Program, St. Boniface General Hospital, Winnipeg, Manitoba, Canada*

[i]*Department of Biosystems Engineering, University of Manitoba, Winnipeg, MB, R3T 2N2, Canada*

[j]*Department of Immunology, University of Manitoba, Winnipeg, MB, R3E 0T5, Canada*

† Electronic supplementary information (ESI) available. See DOI: 10.1039/c4ra12863j

targeted organs and heterogeneous cell populations used in the studies. Meyerrose *et al.* administered transduced ASCs to sublethally irradiated immune deficient mice through various routes (*e.g.* intravenous, intraperitoneal or subcutaneous injection). Seventy-five days after transplantation, the administered cells were found in various tissues.[16] Tracing the transplanted stem cells shows that the cells also reached other organs in addition to the target site.[17] Therefore, it is important to explore the potential to control trafficking of stem cells and to develop a technique for selection of stem cells with an effective and specific homing property. Toward this direction, this study was designed to develop a method to select high chemotactic ASCs *in vitro*.

Conventional migration assays such as transwell assay can be used to measure chemotaxis and collect migrated cells.[14,18–20] However, transwell assay has limitations in controlling the chemical gradient and in distinguishing true responding cells from those moving randomly. In contrast, our approach employs a microfluidic platform that allows us to precisely control a chemical gradient and to quantitatively assess cell chemotaxis. Thus, this platform may be used for screening effective chemoattractants for a specific type of stem cells. Subsequently, this approach may also be employed to harvest the stem cells that display a chemotactic property. Previously, Takayama *et al.* demonstrated that parallel streams of different solutions at low Reynolds number can effectively create patterns of the substrate and cells.[21] Similar method was used to pattern endothelial cells for wound healing assays.[22] However, to our best knowledge, those previous studies have not been used to separate and extract high chemotactic and low chemotactic cell populations. In addition, the use of microfluidic devices to manipulate migratory ASCs has not been reported. Using a microfluidic gradient generator, we have shown the characteristic movement of rat ASCs to a defined gradient of epidermal growth factor (EGF).[23] In the present study we further developed a microfluidics-based method to provide an integrated solution for on-chip cell patterning, chemotaxis assay and extraction of chemotactic ASCs. We found that the chemotactic ASCs to EGF could be readily extracted using our method. Subsequently, we assessed the chemotactic property of the selected cells and explored potential mechanisms underlying the chemotactic property.

Materials and methods

1. Cell preparation

Subcutaneous adipose tissues were isolated from the inguinal region of the inbred Lewis rats. ASCs were isolated following the method as described previously.[24] The isolated adipose tissue was washed extensively with phosphate-buffered saline (PBS) to remove contaminating debris and blood cells. The adipose tissue was minced and digested with collagenase I (2 mg mL^{-1}; Worthington Biochemical, Lakewood, NJ) at 37 °C for 20–30 minutes. Collagenase activity was then neutralized by DMEM-low glucose (HyClone, Logan, UT) containing 15% fetal bovine serum (FBS; HyClone, Logan, UT). The digested adipose tissue was filtered with a 100 μm and then with a 25 μm nylon membranes, to eliminate the undigested fragments. The cellular suspension was centrifuged at 1000*g* for 10 min. The cell pellets were re-suspended in cell culture medium and cultivated for 48 h at 37 °C in 5% CO_2. Adherent cells were disassociated with 0.25% trypsin and collected for subsequent studies. The isolated ASCs were cultured and passaged in complete culture medium (DMEM with 10% FBS, 1% penicillin–streptomycin, 1% MEM/NEAA, and 20 ng mL^{-1} EGF) at 37 °C in the presence of 5% CO_2.

2. Microfluidic device preparation

A previously developed "Y" shaped microfluidic gradient-generating device was used for this study.[25–27] The device design was drawn using the Freehand software 9.0 (Macromedia, CA) and plotted onto a transparency sheet. The device master was fabricated using a Si wafer and SU-8 photoresist (Microchem, MA) by the standard contact photolithography. The master was then used to make the polydimethylsiloxane (PDMS) (Dow Corning, MI) replica by the standard soft-lithography technique. Two 1 mm diameter holes for fluidic inlets and one 4 mm diameter hole for the outlet were punched out of PDMS. Then PDMS was bonded to a glass slide using an air plasma cleaner (PDC-32 G, Harrick, NY) to complete the microfluidic device.

3. On-chip cell patterning, chemotaxis and extraction

The microfluidic channels were coated with fibronectin (BD Biosciences, MA) for one hour at room temperature. ASCs were seeded to the device and allowed to settle on the fibronectin-coated channel uniformly for a few hours in an incubator at 37 °C with 5% CO_2. The seeded ASCs were then exposed to a step gradient of trypsin/EDTA (0.25%), which was created by infusing medium and trypsin/EDTA solution into the channel through separate inlets at a total flow rate of 1.2 μL min^{-1} using a syringe pump (KDS210, KD Scientific, MA). The ASCs exposed to trypsin/EDTA were washed out in 5–8 min and those subjected to medium remained firmly on one half of the channel (Fig. 1A). As a result, one half of the channel was loaded with the ASCs while another half in general was ASCs-free. The ASCs remained in the device were then exposed to a smooth concentration gradient of EGF (recombinant human EGF, Cedarlane, Burlington, Ontario) (Fig. 1B). The concentration gradient was created simply by slowly (total flow rate of 0.4 μL min^{-1}) infusing EGF-containing medium (20 ng mL^{-1}) and EGF-free medium (with two syringes) into the device through separate inlets. Chemotaxis of ASCs to the EGF gradient in the microfluidic device was monitored using an inverted microscope (Nikon Ti-U system) with an environmental chamber with its temperature and CO_2 level set at 37 °C, and 5%, respectively. Time-lapse images of cell migration were taken at a frequency of 1 frame per 20 min for up to total 24 h. At the end of the chemotaxis experiment, cells migrated to the high EGF concentration region of the channel were washed off from the channel by applying a step gradient of trypsin/EDTA. The ASCs being washed out were then collected at the outlet (Fig. 1C). We call these cells "high chemotactic cells" or "HC". The ASCs

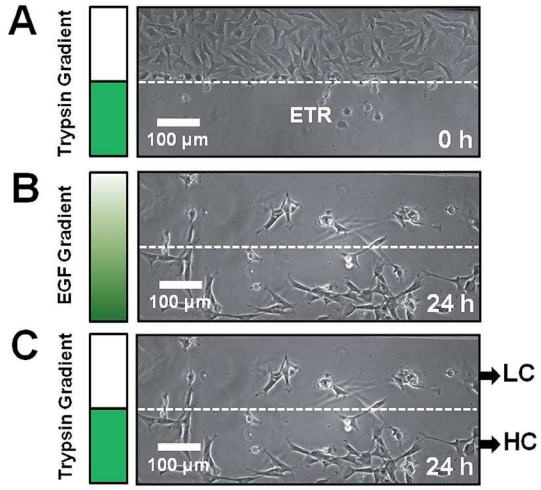

Fig. 1 Illustration of on-chip chemotactic cell selection method. (A) Using a step-gradient of trypsin/EDTA to pattern ASCs in the upper half of the microfluidic channel. ETR indicates the extraction target region. (B) Applying an EGF gradient to induce chemotaxis of patterned ASCs for 24 h. (C) Using a step-gradient of trypsin/EDTA to extract ASCs migrated into the ETR.

remained in the low EGF concentration region of the channel were washed off from the channel by applying a uniform flow of trypsin/EDTA and collected at the outlet (Fig. 1C). We call these cells "low chemotactic cells" or "LC". The extracted HC and LC were cultured for subsequent studies. To further compare chemotaxis of the extracted HC and LC, we fluorescently labeled HC (or LC) with cell tracker dye (CellTracker™ Orange, Life Technologies, CA) and mixed them with LC (or HC) in 1 : 1 ratio (Fig. 4). The same number of the cell mixture was loaded to the device for each experiment. Then the cell mixture was tested for chemotaxis to the EGF gradient following the same procedure as illustrated in Fig. 1.

4. Cell tracking analysis

The cells in the time-lapse images were manually tracked using the "Manual Tracking" plug-in in the NIH ImageJ software (v.1.34s). The cell tracking data were imported to Chemotaxis and Migration Tool software (ibidi, Martinsried, Germany) to compute Chemotactic Index (C.I.) and average cell speed. Chemotactic Index (C.I.) is defined as the ratio of the displacement of cells toward the chemokine gradient (Δy), to the total migration distance (d) using the equation C.I. $= \Delta y/d$, presented as the average value $\pm$ standard error of the mean (SEM). The average speed (V) is calculated as $d/\Delta t$ and presented as the average value $\pm$ SEM of all cells. Furthermore, statistical analysis of migration angles was performed using Origin software (Origin 8.5, Northampton, MA) to examine the directionality of the cell movement. Specifically, migration angles, calculated from x–y coordinates at the beginning and the end of the cells tracks, were summarized in a direction plot, which is a rose diagram showing the distribution of angles grouped in defined intervals with the radius of the wedge indicating the cell number. The most inner circle represents 1 cell with an increment of 1 for the outer circles. Total 20–40 cells were analyzed in each experiment and at least 3 independent experiments (each using a separate device) were repeated for each condition with similar results. The figures show the data from one representative experiment for each condition.

5. Reverse transcription-PCR for measuring gene expression of epidermal growth factor receptor (EGFR)

Total RNA of HC and LC were extracted using the trizoilation method. cDNA were synthesized from the total RNA followed by reverse transcription. The cDNA was then used to amplify EGFR gene by PCR with 35 cycles. The sequences of the primers for rat EGFR were 5′ CTCCTCTAGACCCACGGGAA 3′ (Forward) and 5′ ATGTTCATGGTCTGGGGCAG 3′ (Reverse). Gene-bank number and product length are NM_031507.1 and 553 bp, respectively. The PCR products were verified on agarose gel. The bands were visualized using a UV illuminator and the corrected band density was measured to indicate EGFR gene expression. Glyceraldehyde-3-phosphate dehydrogenase (GAPDH) was used as an internal control. Each RT-PCR experiment was performed in triplicate. The figure presents the average data from all repeats with the error bar as the standard error of the mean (SEM).

6. Flow cytometry

6.1. Surface EGFR expression. HC and LC were serum starved in EGF-free culture medium overnight. Then the cells were stimulated by 50 ng mL^{-1} of EGF for 3 h. The stimulated cells were fixed in 2% paraformaldehyde (PFA) and stained with EGFR antibodies following the manufacturers' instructions. The primary EGFR antibody was purchased from Santa Cruz Biotechnology. The secondary Alexa Fluor 488 antibody was purchased from Life Technologies. The stained cell samples were analyzed for surface EGFR expression using a flow cytometer (FACSCalibur, BD Biosciences, ON). The FACS data were analyzed using FlowJo (7.2.5 Tree Star Inc, OR). The relative EGFR expression level was computed as the fold change of mean fluorescence intensity of the EGFR staining signal to the negative control without primary antibody staining. The figure presents the average data from 3 independent experiments with the error bar as the standard error of the mean (SEM).

6.2. Phospho FACS for measuring Erk1/2 phosphorylation. Erk1/2 phosphorylation in HC and LC were measured by phospho FACS following a similar method as described previously.[28] HC and LC were serum starved in EGF-free culture medium overnight. Then the cells were stimulated by 50 ng mL^{-1} of EGF for 3 h. The stimulated cells were fixed in 2% PFA and subsequently permeabilized in 100% ice-cold methanol overnight at -20 °C. The permeabilized cells were washed twice with staining buffer (0.5% BSA in PBS) followed by intracellular staining using the phospho Erk1/2 antibodies (Alexa Fluor 647 Conjugate phospho-p44/42 MAPK (Erk1/2) Rabbit mAb, New England Biolabs, ON). The stained cell samples were analyzed for Erk1/2 phosphorylation using a flow cytometer (FACSCalibur, BD Biosciences, ON). The FACS data were analyzed using FlowJo. The relative Erk1/2 phosphorylation level was computed

as the fold change of mean fluorescence intensity of the Erk1/2 staining signal to the negative control without Erk1/2 antibody staining. The figure presents the average data from 3 independent experiments with the error bar as the standard error of the mean (SEM).

7. Statistical test

Statistical data analysis was performed using Origin software. Two-tailed student's *t*-test was used for two-group data comparison. The significance level is defined as: $p < 0.05$ (*); $p < 0.01$(**); $p < 0.001$(***). A *p*-value <0.05 was considered statistically significant.

Results

1. On-chip selection of chemotactic ASCs

The key objective of the on-chip cell selection method is to extract the cells that are able to migrate towards a higher concentration region of the chemoattractant gradient. We call this high chemoattractant region the "Extraction Target Region" (ETR). In our previous study, ASCs were randomly seeded in the microfluidic channel for chemotaxis experiment.[23] The random cell seeding makes it difficult to separate the cells that migrated into the ETR from the cells that were initially seeded in the ETR. For this reason, we patterned ASCs on one half of the channel by applying a step-gradient of trypsin/EDTA to remove the cells in the other half of the channel, which is the ETR in this method (Fig. 1A). We found this cell patterning method is simple and fast. We anticipate that this method can be generally useful for patterning adherent cells.

In the next step, we tested if the seeded ASCs can migrate more directionally toward a chemical gradient that will allow subsequent extraction of the chemotactic cells from the ETR. Considering the slow migration speed of ASCs (several μm h^{-1} to a few tens μm h^{-1}) and the relatively large dimension of the gradient region (a few hundred μm),[23] we followed ASCs migration for 24 h (20 min/frame) to allow significant cell migration into the ETR. In our previous study, we demonstrated chemotaxis of ASCs to an EGF gradient using the microfluidic device.[23] In the present study, we apply the same EGF gradient for proof-of-concept.

In this study, the 20 ng mL^{-1} EGF solution and media alone were infused into the microfluidic channel through separate inlets. Then the two flows diffuse into each other by continuous laminar flow mixing to develop an EGF gradient across the channel width. Therefore, the gradient is stable over time. The gradient stability was checked over the cell migration experiment. Depending on the exact position along the length of the channel, the gradient profile can be different. Over each 0.8 mm length scale under our experimental conditions, the gradient profile was identical as characterized previously.[25] As shown in Fig. 2 (data from a different experiment than it in Fig. 1 and 3), cells in most regions below the Y junction along the 10 mm long channel clearly migrated towards the EGF gradient. We chose the region between 3 mm and 3.8 mm below the Y junction consistently for all analysis.

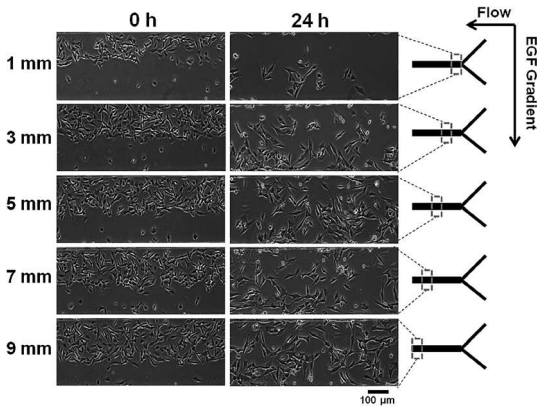

Fig. 2 ASCs in different regions along the length of the channel during chemotaxis experiment to EGF. The left panel shows the patterned ASCs at 0 h of the chemotaxis experiment in different regions below the Y junction in the microfluidic channel. The middle panel shows the corresponding regions at the end of the 24 h chemotaxis experiment. The right panel illustrates the corresponding regions in the Y device and the directions of flow and EGF gradient.

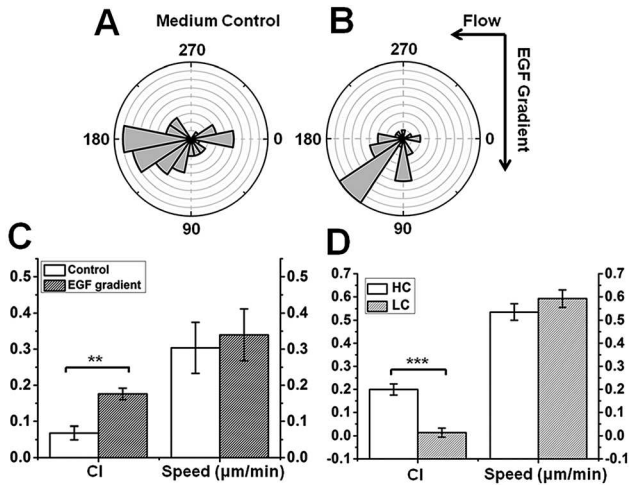

Fig. 3 Comparison of ASCs migration in an EGF gradient and in medium control and comparison of chemotaxis to the EGF gradient between HC and LC. (A and B) Angular histogram show more cells migrated toward the EGF gradient and comparable number of cells moving upwards and downwards in the medium control. (C) ASCs in the EGF gradient has a higher Chemotactic Index than in the medium control. The cell migration speed is comparable under both conditions. (D) HC has higher Chemotactic Index to the EGF gradient than LC. The cell migration speed is comparable between HC and LC.

Because the cells were patterned in one half of the channel, the cells tend to spread into the ETR, where more space is available, even in the absence of a gradient. To reduce this bias effect on comparing cell migration with or without a gradient, we took the starting time point a few hours after the migration experiment. More specifically, the starting time point was chosen when cells were observed to uniformly distribute in the entire channel in an EGF gradient or in the

medium control. We consistently chose this time point 3–4 h after the migration experiment began. The less than 1 h variation among different experiments is small comparing to the total 24 h cell migration experiment. When we compared the migration in an EGF gradient and in medium control using the entire cell migration period (including the initial 3–4 h), we found higher Chemotactic Index in an EGF gradient comparing to the medium control. However, this difference is not statistically significant. Excluding the first 3–4 h helps reduce the effect of the cell's tendency to occupy the empty space in the channel, which is in the direction toward the EGF gradient. Indeed, this modified analysis enhanced the difference of Chemotactic Index between EGF gradient and medium control.

Comparing to control medium without an EGF gradient, we found more ASCs migrated toward the EGF gradient as shown by the angular histogram analysis (Fig. 3A and B). Consistently, 83% of the cells migrated towards the EGF gradient whereas only 60% of the cells migrated downward in the control medium. ASCs show a significantly higher Chemotactic Index (C.I.) in the EGF gradient whereas the cell speed is comparable under both conditions (Fig. 3C). Furthermore, many ASCs reached the bottom region of the EGF gradient, where the EGF concentration is higher, at the end of the 24 h chemotaxis experiment (Fig. 1B and 2). Taken together, the EGF gradient effectively induced chemotaxis of a sub-population of ASCs into the ETR. We call the ASCs migrated into the ETR the "high chemotactic cells" (HC) (Fig. 1C). By contrast, we call the cells remained in the upper half of the channel at the end of the chemotaxis experiment the "low chemotactic cells" (LC) (Fig. 1C).

To extract HC, a step gradient of trypsin/EDTA was applied to wash off cells in the ETR from the channel and these cells were then collected at the outlet (Fig. 1C). Afterwards, LC in the low EGF concentration region of the gradient (upper half of the channel) were washed off from the channel by applying a uniform flow of trypsin/EDTA and collected at the outlet. The extracted HC and LC were cultured for further studies. This step-gradient of trypsin/EDTA-based method was found effective for separation and collection of cells of interest.

To confirm that HC has higher level of chemotaxis than LC, we compared C.I. between HC and LC with the same chemotaxis experiments. We found that HC had significantly higher C.I. than LC. Consistently, 100% of HC but only 40% of LC migrated towards the EGF gradient. However, their migration speed was comparable (Fig. 3D). Because cells were patterned over the upper half of the channel, their initial positions were not the same relative to the ETR. Therefore, it would be easier for cells initially seeded closer to the ETR to migrate into the ETR. If this was the case, HC or LC would not be truly high or low chemotactic cells as we expected. In this study, however, we found that the initial positions between HC and LC is statistically indistinguishable ($p = 0.89$ in t-test). Therefore, we can rule out the possibility that the higher directional migration of HC to the EGF gradient than LC is due to their initial closer positions relative to the EGF gradient. These results proved the validity of our on-chip cell selection strategy.

2. Validation of selected chemotactic ASCs

The results described above demonstrated that chemotactic cells could be readily separated from non-chemotactic ones and harvested with our microfluidic platform. However, since the extracted cells went through multiple steps during separation and extraction procedures in microfluidic device, their viability and chemotactic property may be lost. In addition, the directly extracted cell number is insufficient for post-extraction analysis. Therefore, we want to give time for the extracted cells to recover from on-chip manipulations and to test if clonally expanded cells still show difference in chemotaxis to EGF. Therefore, we performed experiments to further assess the proliferation and chemotactic movement of the extracted ASCs. We found that the extracted HC and LC proliferated well under the normal culture condition and were able to produce sufficient clones for further experiments. Next, we tested the migration of mixture of HC and LC to the EGF gradient using the microfluidic device one week after extraction and expansion. Fluorescent labeling of one cell population (HC or LC) allowed us to distinguish HC and LC in the cell mixture (Fig. 4A). This design avoided possible variations (*e.g.* device, gradient condition, growth phase of cells, *etc.*) between separate experiments to test HC and LC. We found that the expanded HC clones maintain the higher chemotactic ability to the EGF gradient comparing with the expanded LC clones. This is shown by the angular histogram analysis and C.I. (Fig. 4B–D). 76% of HC and 48% of LC migrated towards

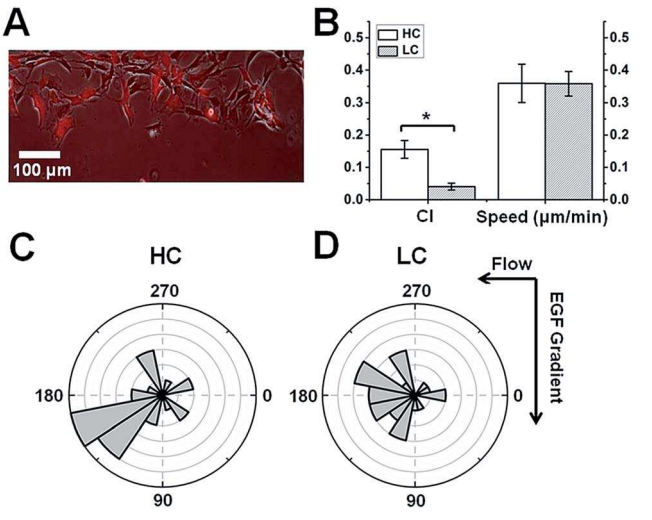

Fig. 4 Validation of the different chemotactic potential to the EGF gradient for HC clones and LC clones. (A) A representative image of mixed HC clones (labeled with cell tracker) and LC clones patterned in a microfluidic channel for chemotaxis experiment to an EGF gradient. (B) HC clones have a higher Chemotactic Index to the EGF gradient than the LC clones. The cell migration speed is comparable between HC clones and LC clones. (C and D) Angular histogram show more HC clones migrated towards the EGF gradient (C) and comparable number of LC clones moving towards and away from the EGF gradient (D).

the EGF gradient respectively. The cell speed was comparable between HC clones and LC clones (Fig. 4B).

3. Characterizations of EGFR signaling in selected ASCs

This on-chip method successfully identified and selected the cell population with higher chemotactic ability to an EGF gradient. Next, it would be useful to elucidate the potential mechanisms underlying the chemotactic ability of HC. The comparable migration speed of HC and LC suggests that the more effective chemotactic migration of HC could not be simply due to the higher motility of HC. Instead, it was our hypothesis that HC have a higher level of messengers and receptors involving in chemotactic signaling than LC in response to the chemoattractant gradient. Since EGF was used as the chemoattractant in this study, we examined the level of EGF receptor in HC and LC. Although RT-PCR results showed no significant difference of EGFR gene expression between HC and LC (Fig. 5A and B), surface EGFR antibody staining and flow cytometric analysis showed that HC had a higher level of the cell-surface EGFR than LC upon 3 h EGF stimulation (Fig. 5C). Immunofluorescence staining and imaging shows qualitative difference of EGFR expression in HC and LC (ESI S1†) Moreover, HC exhibited a higher phosphorylation level of extracellular signal-regulated kinases 1/2 (Erk1/2) than LC upon 3 h EGF stimulation (Fig. 5D and ESI S2†). EGF stimulation for 1 h or 2 h showed no significant difference in surface EGFR expression and Erk1/2 activation between HC and LC. Serum and EGF starvation and a higher dose of EGF stimulation meant to enhance the difference of EGFR expression and activation between HC and LC. 50 ng mL^{-1} of EGF for EGFR signaling studies is a very low concentration relative to those used by others in assessment of EGFR signal pathway. It is expected that effects of EGF at 50 ng mL^{-1} would not significantly differ from those at 20 ng mL^{-1}. Taken together, although HC and LC have similar EGFR gene expression in the resting state, the EGF increased HC's expression of cell-surface EGFR and enhanced phosphorylation of Erk1/2 in the downstream of EGFR signaling pathway. As a result, we believe that activation of EGFR signalling pathway may be responsible for the higher chemotactic ability of HC to the EGF gradient.

Discussion

ASCs are typically defined by a panel of protein markers.[12] Previous study showed that human ASCs express the receptors for a range of chemotactic factors ranging from growth factors to chemokines. Chemotactic capacity of human ASCs to these chemotactic factors have been assessed *in vitro* using conventional transwell assays.[14] Similar chemotactic potential may be shared by ASCs from vertebrate and rodent origins. However, the migratory properties of ASCs used for transplantation has not been characterized. It is likely that the ASCs consist of highly heterogeneous migratory and chemotactic phenotypes. Separating chemotactic stem cells from non-chemotactic stem cells and harvesting the chemotactic ones will have a great potential to increase the homing of transplanted ASCs to target organs improving the outcome of cell therapy. The microfluidic method established in this study integrates cell patterning, chemotaxis, and cell harvest on a single chip. The concentration gradient generator used in this study can flexibly produce a stepwise gradient of trypsin/EDTA for cell patterning and extraction or a smooth chemoattractant gradient for chemotaxis

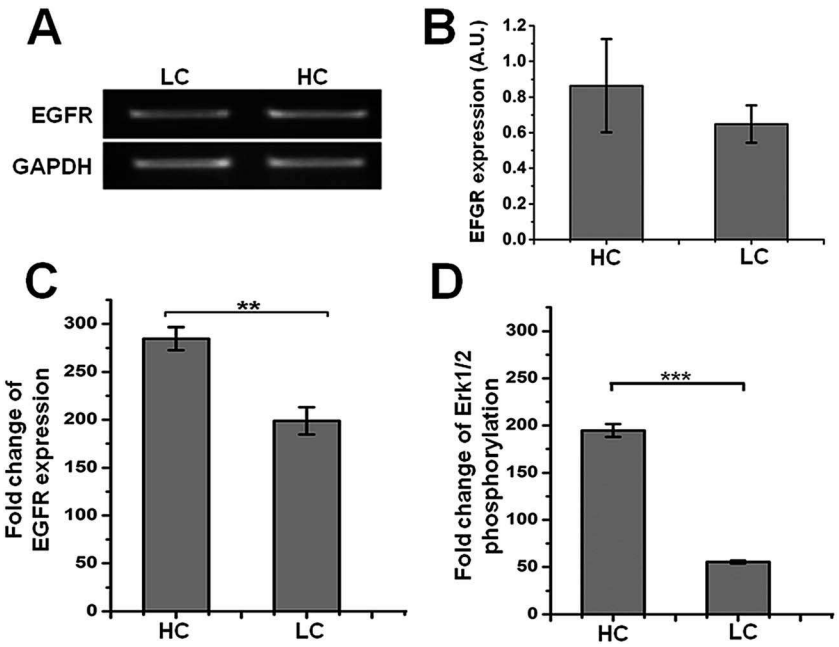

Fig. 5 Characterizations of EGF signaling for HC clones and LC clones. (A and B) RT-PCR analysis shows comparable EGFR gene expression between HC clones and LC clones. GAPDH was used as an internal control. (C) Flow cytometric analysis shows that HC clones has higher surface EGFR expression than LC clones upon EGF stimulation. (D) Phospho flow cytometric analysis shows that EGF triggers higher level of Erk1/2 phosphorylation in HC clones than LC clones.

experiment. Our results demonstrate that such a simple method can be used to extract the cells of interest from heterogeneous cell populations. Moreover, the selected cells preserve their chemotactic property and viability following *ex vivo* expansion. Furthermore, our results suggest that EGFR signaling pathway may be involved in the chemotactic migration of ASCs observed in this study. Thus, targeting the corresponding receptor signaling in ASCs for the target chemoattractant may improve ASC homing for transplantation applications (*e.g.* over-expressing the receptor in ASCs to the chemoattractant identified in the target tissues).

In the current study, we used the previously characterized EGF gradient to demonstrate this on-chip chemotactic ASCs selection method. Evidently, this approach can also be used to select chemotactic ASCs responding to other chemoattractants or other types of chemotactic stem cells (*e.g.* human ASCs as described in ESI S3†). In additional to using known chemoattractants, unknown attractant sources such as supernatant derived from injured tissues can be investigated in this method to select chemotactic stem cells specific to target organs (ESI S4†). Thus, we believe that the cell selection strategy developed in this study has a very wide range of applications and use of this technique may significantly improve outcomes of cell therapy.

On the other hand, the current method definitely has room for improvement, especially in its performance and capability. First, the cell patterning technique can be optimized (*e.g.* determine the optimal trypsin/EDTA concentration and infusion time) to ensure complete removal of cells in the ETR. Second, the cell selection step may need to be repeated to further select the high chemotactic cell population. Moreover, this method can be improved so that chemotactic cells sensitive to multiple chemotactic factors can be harvested. Third, the current version of our microfluidic chip can be improved to increase the throughput of cell selection and harvest. This can be achieved by integrating a large number of cell selection modules on a single chip, which will not only allow large-scale cell selection, but also avoid possible phenotypic or/and genotypic changes of the selected cells during expansion. Moreover, large-number cell-selection modules will also permit simultaneous selections of different cell populations. Finally, new techniques can also be used to obtain single cell populations for biological studies. Possible strategies for single cell selection may include using a microfluidic microinjector to locally detach a target cell,[29,30] or using a microfluidic "racing" design to select the fastest cell to reach the chemoattractant source.[31,32] In conclusion, our developed microfluidic strategy is effective in selection and harvest of chemotactic cells to chemoattractants of interest. It is our expectation that use of this approach can significantly improve therapeutic benefits of stem cells.

Acknowledgements

This study is supported by a Discovery Grant from the Natural Sciences and Engineering Research Council of Canada (NSERC) to F. Lin, and a CIHR emerging team grant for regenerative medicine and nanomedicine. F. Lin thanks the Winnipeg Rh Institute Foundation and the University of Manitoba for a Rh Award; K. Natarajan thanks the Faculty of Science and the Faculty of Graduate Studies at University of Manitoba for graduate fellowships.

References

1 J. Seita and I. L. Weissman, *Wiley Interdiscip. Rev.: Syst. Biol. Med.*, 2010, **2**, 640–653.
2 J. J. Chong and C. E. Murry, *Stem Cell Res.*, 2014, **13**, 654–665.
3 K. A. Choi, I. Hwang, H. S. Park, S. I. Oh, S. Kang and S. Hong, *Biotechnol. J.*, 2014, **9**, 882–894.
4 B. G. Chung, L. A. Flanagan, S. W. Rhee, P. H. Schwartz, A. P. Lee, E. S. Monuki and N. L. Jeon, *Lab Chip*, 2005, **5**, 401–406.
5 F. Li and S. Z. Zhao, *World J. Stem Cell*, 2014, **6**, 296–304.
6 W. Tsuji, J. P. Rubin and K. G. Marra, *World J. Stem Cell*, 2014, **6**, 312–321.
7 P. A. Zuk, M. Zhu, P. Ashjian, D. A. De Ugarte, J. I. Huang, H. Mizuno, Z. C. Alfonso, J. K. Fraser, P. Benhaim and M. H. Hedrick, *Mol. Biol. Cell*, 2002, **13**, 4279–4295.
8 J. M. Gimble, *Expert Opin. Biol. Ther.*, 2003, **3**, 705–713.
9 J. M. Gimble and F. Guilak, *Cytotherapy*, 2003, **5**, 362–369.
10 A. Schäffler and C. Büchler, *Stem Cells*, 2007, **25**, 818–827.
11 A. M. Rodriguez, C. Elabd, E.-Z. Amri, G. Ailhaud and C. Dani, *Biochimie*, 2005, **87**, 125–128.
12 L. Wang, J. Deng, W. Tian, B. Xiang, T. Yang, G. Li, J. Wang, M. Gruwel, T. Kashour, J. Rendell, M. Glogowski, B. Tomanek, D. Freed, R. Deslauriers, R. C. Arora and G. Tian, *Am. J. Physiol.: Heart Circ. Physiol.*, 2009, **297**, H1020–H1031.
13 H. Mizuno, *J. Nippon Med. Sch.*, 2009, **76**, 56–66.
14 S. J. Baek, S. K. Kang and J. C. Ra, *Exp. Mol. Med.*, 2011, **43**, 596–603.
15 A. Sohni and C. M. Verfaillie, *Stem Cells Int.*, 2013, **2013**, 130763.
16 T. E. Meyerrose, D. A. De Ugarte, A. A. Hofling, P. E. Herrbrich, T. D. Cordonnier, L. D. Shultz, J. C. Eagon, L. Wirthlin, M. S. Sands, M. A. Hedrick and J. A. Nolta, *Stem Cells*, 2007, **25**, 220–227.
17 Y. Saito, M. Shimada, T. Utsunomiya, T. Ikemoto, S. Yamada, Y. Morine, S. Imura, H. Mori, Y. Arakawa, M. Kanamoto, S. Iwahashi and C. Takasu, *J. Hepatobiliary Pancreat. Sci.*, 2014, **21**, 873–880.
18 R. D. Nelson, P. G. Quie and R. L. Simmons, *J. Immunol.*, 1975, **115**, 1650–1656.
19 S. Zigmond, *J. Cell Biol.*, 1977, **75**, 606–616.
20 A. Lohof, M. Quillan, Y. Dan and M. Poo, *J. Neurosci.*, 1992, **12**, 1253–1261.
21 S. Takayama, J. C. McDonald, E. Ostuni, M. N. Liang, P. J. Kenis, R. F. Ismagilov and G. M. Whitesides, *Proc. Natl. Acad. Sci. U. S. A.*, 1999, **96**, 5545–5548.
22 A. D. van der Meer, K. Vermeul, A. A. Poot, J. Feijen and I. Vermes, *Am. J. Physiol.: Heart Circ. Physiol*, 2010, **298**, H719–H725.
23 N. Wadhawan, H. Kalkat, K. Natarajan, X. Ma, S. Gajjeraman, S. Nandagopal, N. Hao, J. Li, M. Zhang,

J. Deng, B. Xiang, S. Mzengeza, D. H. Freed, R. C. Arora, G. Tian and F. Lin, *Lab Chip*, 2012, **12**, 4829–4834.
24 E. Elhami, A. Goertzen, B. Xiang, J. Deng, C. Stillwell, S. Mzengeza, R. Arora, D. Freed and G. Tian, *Eur. J. Nucl. Med. Mol. Imaging*, 2011, **38**, 1323–1334.
25 F. Lin and E. C. Butcher, *Lab Chip*, 2006, **6**, 1462–1469.
26 F. Lin, in *Methods in Enzymology*, ed. M. H. Tracy and J. H. Damon, Academic Press, 2009, vol. 461, pp. 333–347.
27 J. C. McDonald and G. M. Whitesides, *Acc. Chem. Res.*, 2002, **35**, 491–499.
28 F. Lin, F. Baldessari, C. Gyenge, T. Sato, R. Chambers, J. Santiago and E. Butcher, *J. Immunol.*, 2008, **181**, 2465–2471.
29 D. Juncker, H. Schmid and E. Delamarche, *Nat. Mater.*, 2005, **4**, 622–628.
30 O. Guillaume-Gentil, T. Zambelli and J. A. Vorholt, *Lab Chip*, 2014, **14**, 402–414.
31 Y. Fu, L. K. Chin, T. Bourouina, A. Q. Liu and A. M. J. VanDongen, *Lab Chip*, 2012, **12**, 3774–3778.
32 Z. Tong, E. M. Balzer, M. R. Dallas, W.-C. Hung, K. J. Stebe and K. Konstantopoulos, *PLoS One*, 2012, **7**, e29211.